Sanja Tunjic, BSc

Graphene and graphene derivatives for antibacterial application and biosensing

MASTER'S THESIS

to achieve the university degree of
Master of Science

Master's degree programme: Biotechnology

submitted to:
Graz University of Technology

Supervisor

Prof. Ivan Mijakovic
Department of Biology and Biological Engineering, Chalmers University of Technology, Gothenburg, Sweden

Assoc. Prof. Harald Pichler
Institute of Molecular Biotechnology, Graz University of Technology, Austria

Graz, October 2017

AFFIDAVIT

I declare that I have authored this thesis independently, that I have not used other than the declared sources/resources, and that I have explicitly indicated all material which has been quoted either literally or by content from the sources used. The text document uploaded to TUGRAZonline is identical to the present master's thesis.

_____ _____

Date Signature

Table of content

Acknowledgments

I would love to thank my supervisor Ivan Mijakovic and my mentors Dr. Raghu Mokkapati and Dr. Santosh Pandit at the Division of Systems and Synthetic Biology of the Department of Biology and Biological Engineering at Chalmers University of Technology. I have been extremely lucky to work on my master's thesis project with people who cared so much about me and my work and made this experience valuable for my future career.
I am also very grateful to Prof. Harald Pichler from Graz University of Technology. Even though we were far away, you were always available. Thank you for all the guidance and support.
I am thankful to Dr. Emanuele Celauro for the necessary support during the experimental work and Ulf Sodervall for the training for the Clean Room.

Zusammenfassung

Der Transfer von Resistenzgenen zwischen pathogenen Bakterienpopulationen reduziert die Wirksamkeit von Antibiotika und verursacht damit weltweit Millionen von Todesfällen. Es besteht dringender Bedarf, neue Ansätze zur Behandlung von Infektionen mit pathogenen Bakterien zu entwickeln. Seit seiner Entdeckung hat das Interesse an der Untersuchung der antibakteriellen Aktivität von Graphen und Graphenderivaten zugenommen, obwohl widersprüchliche Ergebnisse von verschiedenen Forschergruppen veröffentlicht wurden. Diese wissenschaftlichen Widersprüche sind auf Variationen in den Parametern Graphen-Flockengröße, -Konzentration, -Herstellungsverfahren, -Dicke und vor allem auf die Art der untersuchten Bakterien zurückzuführen.

In der vorliegenden Arbeit wurde die antibakterielle Aktivität von mit Bor-Atomen dotiertem Graphen (B-G) gegenüber drei Bakterienstämmen untersucht: grampositiver *Staphylococcus epidermidis*, gramnegative *Pseudomonas aeruginosa* und *Escherichia coli*. Es wurde festgestellt, dass B-G weder bakterizid noch bakteriostatisch für irgendeine Art der getesteten Bakterienstämme ist. Der antibakterielle Effekt war auch nicht abhängig von der Art des Substrats, auf dem B-G vorlag (Leiter, Halbleiter oder Isolator). Andererseits wurde beobachtet, dass B-G die Sekretion von Exotoxin A durch *P. aeruginosa* verstärkt.

Auch für andere 2D-Materialien wie WS_2 (Wolframdisulfid) und MoS_2 (Molybdändisulfid) wurde keinerlei antibakterielle Wirkung auf die oben erwähnten Bakterienstämme gefunden. Silber (Ag) und Gold (Au) Nanopartikel von *Cannabis sativa* (Hemp) wurden auf ihre bakteriostatische oder bakterizide Wirkung getestet. Silbernanopartikel zeigen eine vielversprechende antibakterielle Wirkung gegen die gramnegativen Bakterien *P. aeruginosa* und *E. coli*.

Neben dem Testen der antibakteriellen Aktivität von verschiedenen Graphenderivaten wurde ein Graphen-basierter Biosensor hergestellt und getestet, um den Schwellenwert der Biofilmbildung von Bakterien zu bestimmen. Dies soll zur Erkennung von Infektionen und zur Reduktion der Infektionswahrscheinlichkeit von Patienten mit Implantaten führen.

Abstract

The rapid transfer of resistance genes between pathogenic bacterial population reduces the antibiotic efficacy, which causes millions of deaths worldwide. There is a need to develop novel approaches for treatment of pathogenic bacteria. Since its discovery, the interest in investigating the antibacterial activity of graphene and graphene derivatives has predominantly increased where contradictory results have been published by various researchers. These contradictions are due to various parameters like flake size, concentration, method of preparation, thickness and most importantly the type of bacteria.

In the current work, antibacterial activity of boron doped graphene (B-G) was examined against three bacterial strains: Gram-positive *Staphylococcus epidermidis*, Gram-negative *Pseudomonas aeruginosa* and *Escherichia coli*. It was realized that B-G is neither bactericidal nor bacteriostatic to any type of tested bacterial strains. Antibacterial effect was also not dependent on the type of substrate B-G was present on (conductor, semiconductor or insulator). On the other hand, an interesting observation was that B-G enhances the secretion of exotoxin A by *P. aeruginosa.*

Other 2D materials like WS_2 (Tungsten disulfide) and MoS_2 (Molybdenum disulfide) were also unsuccessfully tested for antibacterial effect on above mentioned bacterial strains.

Silver (Ag) and gold (Au) nanoparticles derived from *Cannabis sativa* (Hemp) were tested for their bacteriostatic or bactericidal activity. Silver nanoparticles show promising antibacterial effect against Gram-negative bacteria *P. aeruginosa* and *E. coli*.

Besides testing antibacterial activity of different graphene derivatives, graphene based biosensor was fabricated and tested to detect the threshold of bacteria biofilm formation. This helps in detection and reducing the infections for the patients with implants.

1. Boron doped graphene for antibacterial applications

1.1. Introduction

1.1.1. Graphene

Carbon is the basic element of organic chemistry and an essential element of life. Due to the flexibility of its bonding, carbon-based systems can be found in different structures with various physical properties such as graphite, nanotubes, nanowires [1]. Graphite is a naturally occurring material, used in everyday life, it is composed of layers of graphene (Fig. 1.1). Graphene is an allotrope of carbon packed into two dimensional (2D), single layer sp^2-hybridized honeycomb crystal lattice [2]. Each carbon atom of pristine graphene is bound to three others in the same plane with a strong carbon-carbon bond. Compared to diamond, graphene is a soft material due to interlayer bonding through weak Van der Waals forces. Graphene can be viewed as a planar aromatic molecule, which consists of layer of π conjugated benzene-like structures. Because of the planar structure and the presence of free π electrons, graphene is capable of immobilizing a large number of substances including biomolecules, drugs, and metals [3]. Since its discovery in 2004 by Andre Geim and Konstantin Novoselov from University of Manchester, graphene became a topic of intense research due its unique electronic, optical, mechanical and biomedical properties [4]. Besides its applications in electronic, optics, aviation and materials among a few to mention, there is a huge interest of using graphene-based nanomaterials for biomedical applications, such as sensing, drug delivery, tissue engineering, medical devices, cancer therapy and antibacterial applications [5].

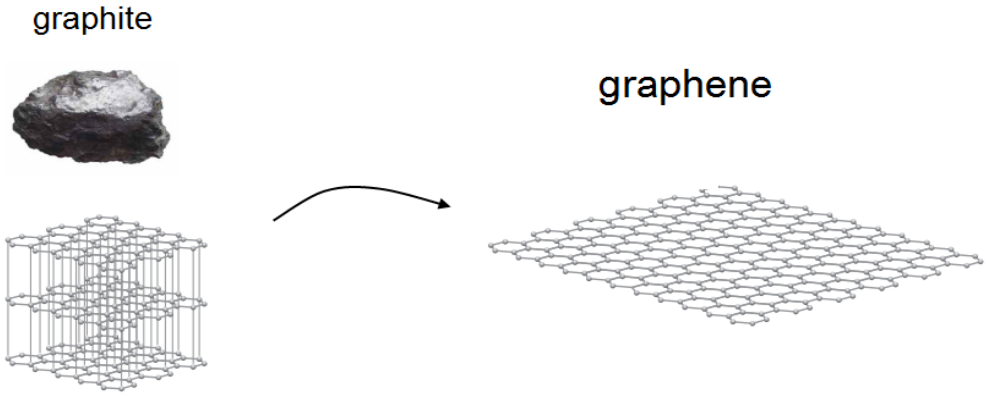

Figure 1.1: Graphite is naturally occurring material composed of many layers of graphene [2].

1.1.2. Chemical vapor deposition (CVD) graphene

Graphene can be prepared by different methods including chemical or mechanical exfoliation, chemical vapor deposition (CVD), Epitaxial growth, Micro-wave assisted oxidation, Ion implantation and by reduction [6]. Among all these methods, CVD graphene has gained prominence as high quality large areas of graphene films can be grown on various metal substrates [7]. CVD process is based on thermal decomposition of the hydrocarbon source on a heated substrate at 1000°C. Due to its catalytic performance, the metal substrate lowers the energy barrier of the reaction. The important parameter is carbon solubility on metal substrate. Metals such as Nickel (Ni) have higher carbon solubility and carbon (C) dissolves into heated substrate. On the other hand, metals with lower carbon solubility such as copper (Cu) are widely used for preparation of large area monolayer graphene. Due to the low solubility of C atoms in Cu, monolayer graphene can grow in a self-limiting process by which graphene can be easily grown on commercially available Cu-foils [8, 9].

1.1.3. Boron doped graphene

The physicochemical properties of pristine graphene nanosheets can be modified by introducing heteroatoms or covalent bonds with specific functional groups to the carbon sp^2 lattice (Fig. 1.2) [10]. This method is known as doping and is the most basic modification of graphene. It is an effective approach to tune its electronic and chemical properties. Various heteroatoms such as Nitrogen (N), Boron (B), Sulfur (S), Selene (Se), Oxygen (O) can be used as dopants, however, boron and nitrogen have attracted the attention of the scientific community the most, due to the similarity of their atomic radii to that of carbon. Doping graphene with N or B creates a band gap and induces n-type or π-type conductivity and promote graphene´s electrical and conductivity properties [11, 12].
Boron is a semiconductor element which has properties between metals and non-metals and is of extremely low abundance compared to that of hydrogen, carbon, nitrogen or oxygen [13]. In plant cells, it plays an essential role together with calcium in cell signaling [14]. Boron is the trace mineral with important role for humans in anti-inflammatory effects, impact on wound healing, bone development and regeneration, regulation and metabolism of sex hormones and vitamin D, absorption of calcium and magnesium, and reduction of heavy-metal toxicity [15].

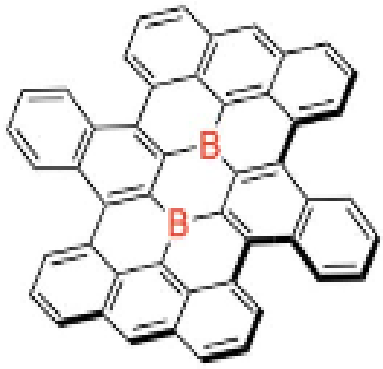

Figure 1.2: Boron doped graphene: Carbon atoms are replaced with Boron [16].

1.1.4. Cytotoxicity of graphene based nanostructures

There are many contradictory results regarding the antimicrobial potential of graphene based materials [17]. Though there has been a lot of literature and hypothesis, the exact antibacterial activity of graphene/graphene derivatives is not clear yet. Most relevant properties affecting antibacterial activity of graphene based materials include surface area, surface chemistry, purity and layer number, methods used for preparation, flake size, type of graphene and most importantly type of bacteria [18]. However, generation of reactive oxygen species (ROS) and oxidative stress induction have been proposed as primary mechanisms of cytotoxicity [19]. Oxygen is necessary for life of most aerobe living organisms, which is also a precursor for ROS generation, that may damage cells and cellular components and can be produced as a result from all forms of cellular toxicity. When in contact with the graphene surface, oxygen forms superoxide intermediates, which oxidize cellular glutathione (GTH) and produce superoxide species. The antibacterial activity can also depend on the conductivity of the substrate on which graphene is deposited [20]. When bacteria come in contact with the sharp edges of graphene flakes, the flakes pierce through the membrane and penetrate causing bacterial death. The other suggested mechanism of cytotoxicity is trapping of bacteria within large aggregated-reduced graphene oxide sheets where the bacteria were killed by suffocation [21].

1.1.5. Biomaterials associated infections (BAI)

Devices and implants inserted into the body provide favorable surfaces for bacterial attachment. Infections of indwelling medical devices are mainly caused by Gram-positive bacteria *S. epidermidis* and *S. aureus* and Gram-negative bacteria *P. aeruginosa* and *E. coli*. An essential element in the pathogenesis of BAI is the formation of biofilms, consisting of bacteria, bacterial products and host proteins on the biomaterial surface [22]. By attaching to the surface, bacteria start producing extracellular polymeric matrix and make three-dimensional structures called biofilms. The extracellular matrix slows down the penetration of antibiotic and nutrients to the inner cell layer. Lack of nutrients results in higher resistance of bacterial cells against antibiotics. Due to inappropriate use of antibiotics, pathogenic bacteria develop resistance genes, which transfer rapidly between bacterial populations. At this stage, the treatment of infections only by antibiotic therapy is not successful and the replacement of implants via surgery cannot be avoided. This process is expensive and painful. Thus, development of novel antibiotic materials is of high importance [23].

1.2. Materials and Methods

1.2.1. Materials

Boron doped graphene (dry powder) was purchased from Graphitene (UK). If not stated differently, all other chemicals used were purchased from VWR BDH Chemicals (UK), EMD Millipore (USA) or Sigma-Aldrich (USA) with the highest purity available.

1.2.2. Boron doped graphene: Experimental work

The antibacterial activity of boron doped graphene was evaluated by colony forming units (CFUs) counting and scanning electron microscopy (SEM). CFUs counting was used for quantitative analysis, while with SEM, morphological changes of bacterial cells in bacterial biofilms were analyzed.

1.2.3. Preparation of boron doped graphene membranes

Ethanol, sodium hypochlorite, acetone, methanol, DMF and DMSO were used as solvents in order to realize the best solvent for uniform boron doped graphene membrane formation. Used solvents and their characteristics are summarized in Table 1.1.

Solution of boron doped graphene flakes (B-G flakes) dispersed in solvent with different concentrations (1, 2 and 4 mg/ml) were sonicated for 30 min (80 kHz, 100 W) using Elmasonic P 30 H (Elma-Hans Schmidbauer GmbH, Singen, Germany) prior to every usage. B-G membranes were initially fabricated by spray coating and standard spin coating methods (Karl Suss, Model: Delta 20/BM, BLE) where it was realized that the membranes were not uniform. In this case Drop casting method proved to be successful where ethanol and deionized water (dH_20) were used in a specific concentration to fabricate uniform B-G membranes on glass coverslips (15 mm, VWR International GmbH, Germany). Just by using B-G solution (B-G flakes dispersed in solvents) it was not possible to fabricate uniform membranes by drop casting due to the stacking of B-G flakes. Addition of dH_20 helps in better dispersibility and uniform distribution of B-G flakes resulting in a more uniform B-G membrane.

1.2.4. Choosing a right solvent and boron doped graphene concentration

The right solvent is the one that promotes uniform distribution of B-G flakes on the glass substrate. Prior to drop casting, glass coverslips were cleaned with acetone and ethanol (70%). Few drops of dH_20 along with few drops of B-G solution were casted on separate coverslips and left overnight for drying, followed by heat treatment (180°C, 2 h). The ratio of dH_20 to one of these B-G solutions was in the range of 1:1 to 1:4. The uniform spreading of B-G flakes depends also on the external conditions such as cleanliness of the glass coverslip. After optical, RAMAN and SEM characterization of the prepared membranes, samples with ethanol (EtOH) provided the most uniform B-G membrane. Additionally, the membranes retained their electrical conductivity and stability after the addition of bacterial suspension. For further experiments, membranes were prepared with B-G in EtOH solution. Glass slides were casted with B-G-EtOH (2.5 µg/ml) and dH_20. First depositing 30 µl dH_20 followed by the addition of 10 µl B-G-EtOH resulted in more homogenous deposition. These samples were used to analyze the antibiotic effect against bacterial and mammalian cells.

Used solvents for B-G membranes and their parameters are summarized in Table 1.1.

Table 1.1: Solvents used for membrane formation with boron doped graphene. ☑ - successful, ☒ - non-successful.

Material	Solvent	Membrane uniformity	Membrane conductivity	Biofilm stability
Boron doped graphene	Ethanol	☑	☑	☑
	Sodium hypochlorite	☒	☒	☒
	DMF	☒	☒	☒
	Acetone	☒	☒	☒
	Methanol	☒	☒	☒
	DMSO	☒	☒	☒

1.2.5. Boron doped graphene membranes on different substrates

Antibacterial activity of boron doped graphene was tested on different substrates. B-G membranes were prepared by drop casting method (as described above) on following substrates: glass, Au, Si and SiO_2.

1.2.6. Bacterial strains and biofilm cultivation

The antibacterial activity of boron doped graphene was tested with *Pseudomonas aeruginosa* PA01 (*P. aeruginosa), Escherichia coli* UTI89 (*E. coli) and Staphylococcus epidermidis* ATCC 35984 *(S. epidermidis)*. All strains are classified as risk group 2 in biosafety guidelines and were grown in LB (Luria Bertani) broth medium at 37°C. The LB agar plates were prepared by dissolving 10 g tryptone, 5 g yeast extract and 15 g of agar in 1 L dH_20. Autoclaved LB agar medium was poured into Petri dishes. The bacterial culture grown overnight was diluted in LB-broth to make an inoculum containing 2-5x10^6 CFU/ml suspension. 200 µl of inoculum was loaded onto B-G membrane on glass coverslips (15 mm) and incubated for 4, 8 and 24 h at 37°C. After incubation, the medium was discarded and the samples were rinsed twice in 0.9% NaCl.

1.2.7. Cultivation of NIH3T3 cells

Mouse fibroblast cells were cultured for 48 h on B-G membranes fabricated on glass substrate (see 1.2.4.) along with their respective controls in the complete growth medium (DMEM with

High Glucose, 4.0 mM L-Glu, sodium pyruvate and 10% iron-fortified Bovine Calf Serum, both from ATCC, UK).

1.2.8. Colony Forming Units (CFUs)

CFU counting was used to analyze the viability of bacteria in the biofilm. The rinsed biofilms were collected in 5 ml of 0.89% NaCl, followed by sonication (20 s, 10 W, Branson 450 digital sonifier, USA) to release the bacterial biofilm from glass coverslips. The homogenized suspension (100 µL) was serially diluted in 0.89% NaCl and plated on LB agar respectively, followed by incubation at 37°C overnight. The number of surviving bacteria in biofilm was determined by counting the number of colonies and calculating the total number of CFU in 5 ml NaCl.

1.2.9. Raman Spectroscopy

Raman spectroscopy is a tool to characterize material properties. The characteristic peaks for carbon based materials in Raman spectra are clearly identified by this technique. The membranes were casted by controlled drop casting method. The flake size of the used B-G is in the range of 0.5 to 5 µm. The final thickness of the fabricated B-G membrane is approximately 100 to 120 microns. These membranes were further used for RAMAN characterization.

1.2.10. Scanning Electron Microscopy (SEM)

For SEM, biofilms were fixed with glutaraldehyde (3%) for 2 h and dehydrated in graded series of ethanol concentrations (40, 50, 60, 70, 80, 90, and 100%; v/v) for 10 min in each solution. The dehydrated biofilms were dried at room temperature for 2 h. Prior to SEM, the samples were coated with gold (5 nm, 5 s, 0.2 kW)) using MS 150 Sputter system (FHR, Anlagenbau GmbH, Germany). SEM imaging was performed using JEOL JSM-6301F Scanning Electron Microscope (USA).

1.2.11. Statistical analysis

Experiments were performed in biological triplicates and data is presented as the mean ± standard deviation. Statistical analysis of the results was estimated by the one-way analysis of

variance (ANOVA), followed by the multiple comparison (Tukey) test. Values at $p<0.05$ were considered as statistically significant.

1.3. Results and Discussion

1.3.1. RAMAN characterization

Raman spectroscopy (Wave length = 532 nm) was used for the characterization of the fabricated B-G membranes. It can be observed that there is a slight shift and broadening of D peak (to 1336 cm^{-1}) in comparison to standard carbon materials (1330 cm^{-1}). B-G shows more intense D peak compared to 2D peak. As seen in the spectrum, the 2D peak is suppressed with the addition of boron (Fig. 1.3) [24].

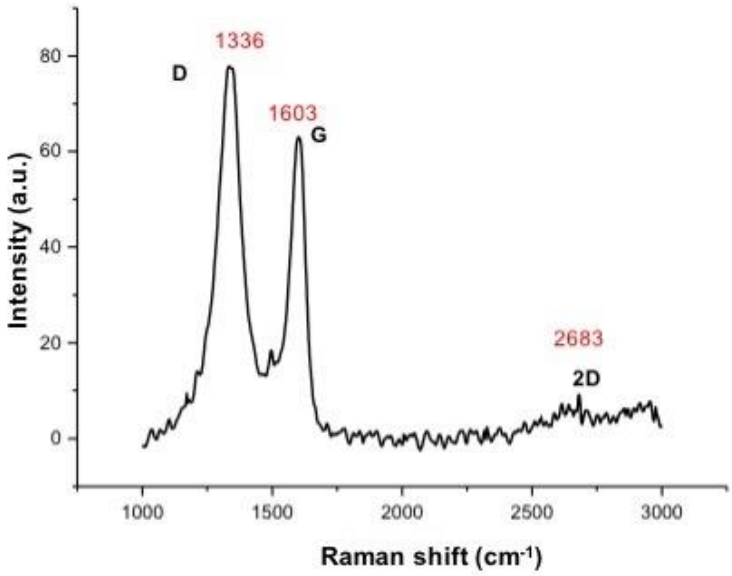

Figure 1.3: RAMAN spectrum of Boron doped graphene membrane.

1.3.2. Membrane integrity

Different solvents were used to fabricate B-G membranes on glass coverslips. Figure 1.4 shows SEM images of B-G membranes prepared with sodium hypochlorite (Klorin, Danmark) and acetone on glass coverslips.

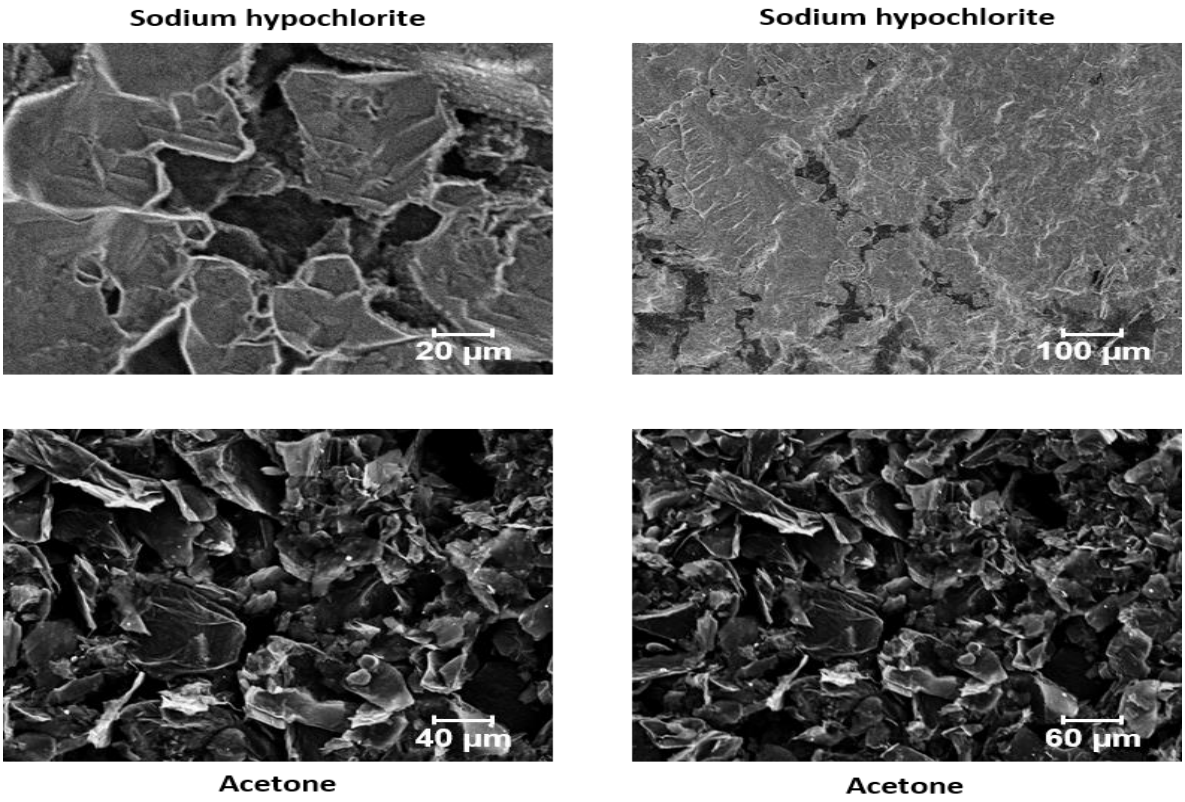

Figure 1.4*:* SEM image of the membrane prepared with B-G + Sodium hypochlorite and B-G + Acetone on glass coverslips.

As seen in Figure 1.4, the membranes prepared with sodium hypochlorite seem to have undergone a chemical reaction where a white layer was observed (this was later proven by the conductivity test where the B-G membranes seemed to have lost their native properties). Figure 1.4 also shows membranes prepared with acetone + B-G, which seem to have uniform coverage on the glass coverslip, nevertheless, when these membranes were immersed in the medium to form a bacterial biofilm, B-G flakes were detached from the membrane and were seen floating within the medium. This is due to the problem of adhesion between acetone B-G flakes and the cover glass surface. Inspite of heat treatment, this acetone based B-G membranes showed similar dispersion within the medium.

The sample prepared with B-G and EtOH is shown in Figure 1.5, which shows membrane uniformity under optical and electron microscopes. When placed in the medium, the membranes were stable without any B-G flake dispersion. Thus, B-G + EtOH membranes were used for all the experiments presented here.

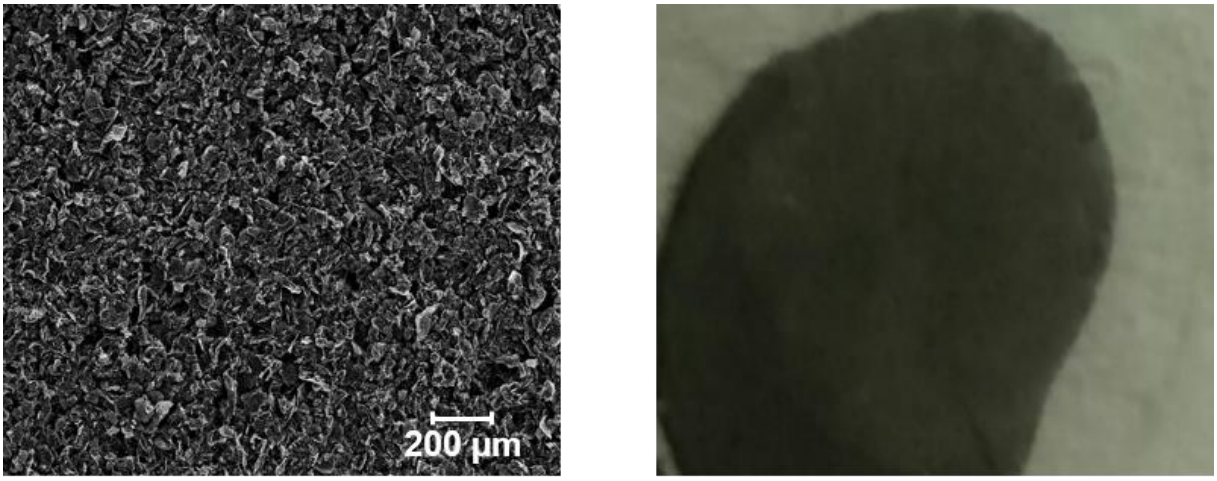

Figure 1.4: SEM (left) and optical (right) analysis of the sample prepared with B-G-EtOH and dH_20 (10 µl:30 µl) showing continuous membrane.

Gram-positive bacteria *S. epidermidis* does not undergo any morphological changes on CVD-graphene (Fig. 1.6) as well as on boron doped graphene (Fig. 1.7). The viability of cells estimated after 4 and 24 h biofilm cultivation on B-G did not show significant difference compared to control sample, which indicates that bacterial cells don't lose viability with increasing incubation time with B-G (Fig. 1.8).

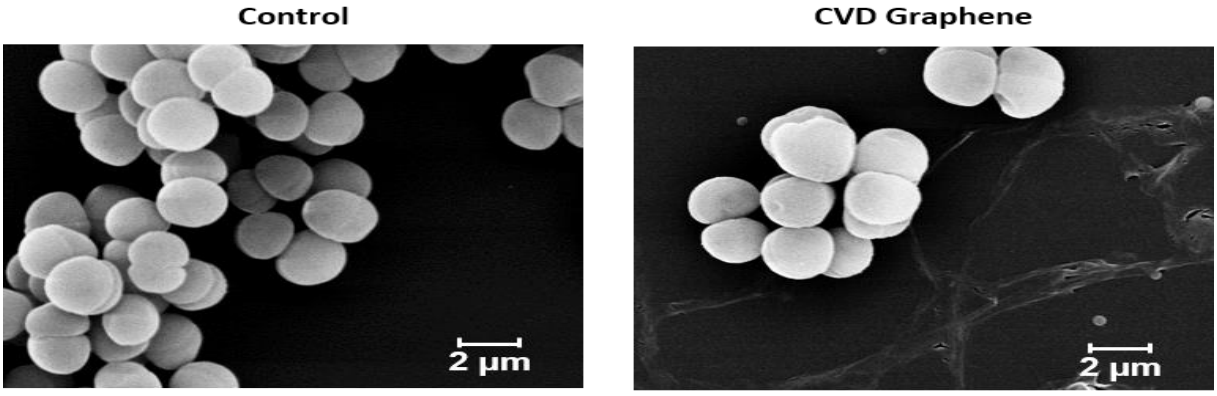

Figure 1.5: SEM imaged of *S. epidermidis* 24 h biofilm on control and CVD graphene. CVD – Chemical Vapour Deposition.

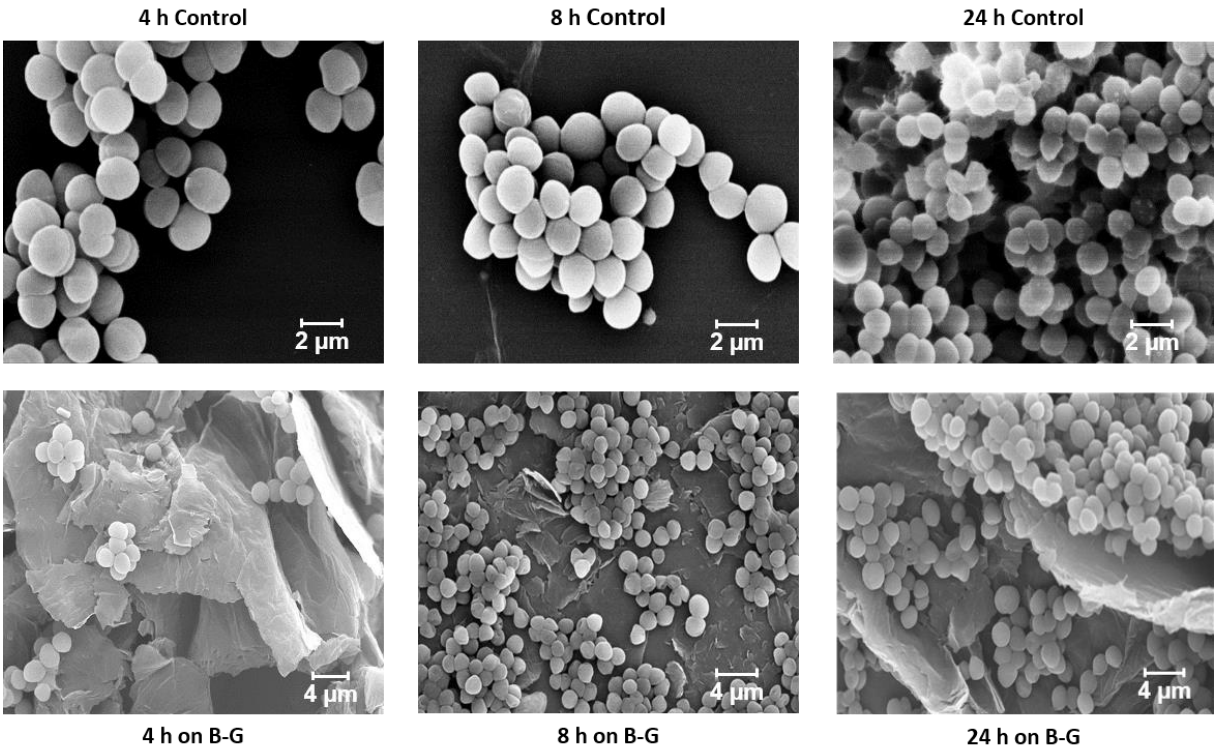

Figure 1.6: SEM images of *S. epidermidis* 4, 8 and 24 h biofilm on control and on boron doped graphene membrane.

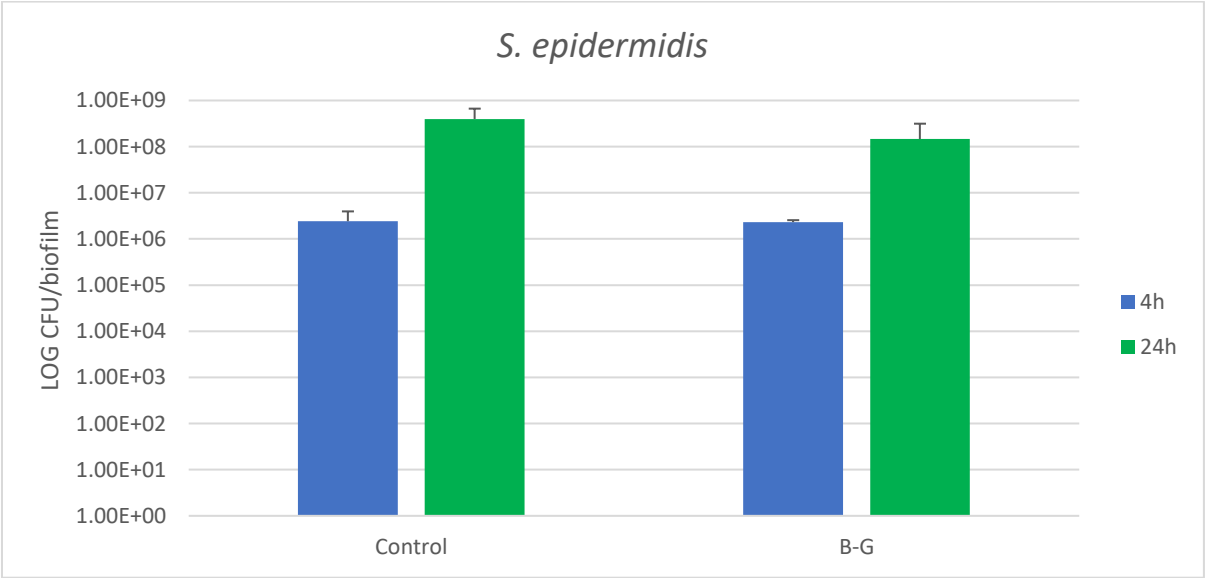

Figure 1.8: The viable *S. epidermidis* cells in 4 and 24 h biofilm on boron doped graphene membrane (B-G) compared to the control samples (glass coverslip).

Boron doped graphene did not have any effect on the morphology and viability of Gram-negative bacteria *P. aeruginosa* and so was the case with Gram-negative *E. coli* (Fig. 1.9, 1.10,). However, in the case of *P. aeruginosa*, B-G was observed to enhance the secretion of EPS (extracellular polymeric substances). The secretion increased with incubation time and was tested till 24 hours (quantification of the secretion was carried out in order to obtain the relation between time and enhanced secretion). Initial experimental data with real time polymerase chain reaction (RT-PCR) suggested that there is an enhanced secretion of tox A by *P. aeruginosa* on B-G substrates. The data was reproducible and has been confirmed multiple times. Detailed experimental data and analysis of tox A secretion will be discussed in Chapter 3. On a side note, tox A is used in cancer and Hepatitis B treatment [25].

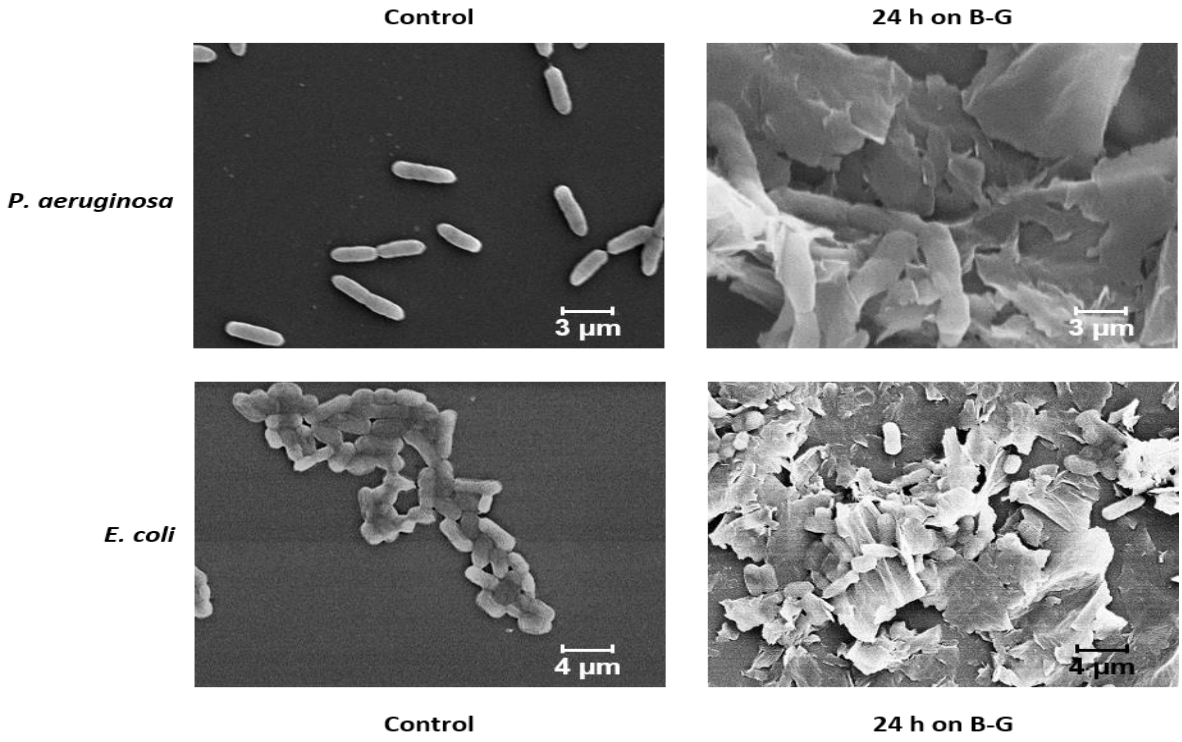

Figure 1.7: SEM images of Gram-negative *P. aeruginosa* and *E. coli* on control and on boron doped graphene membrane.

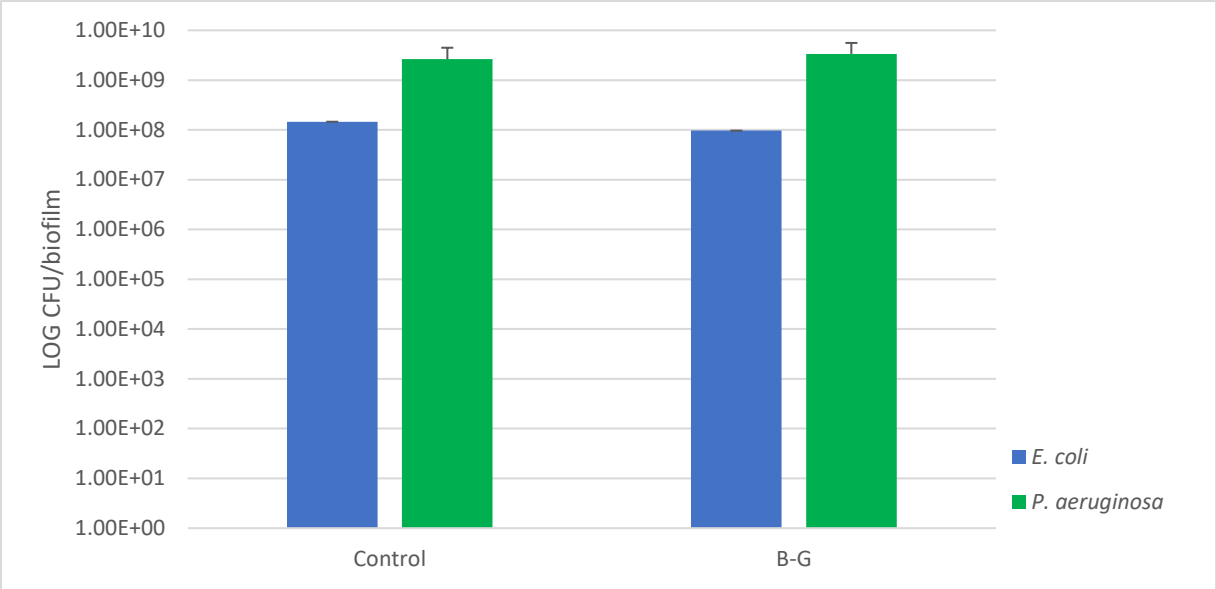

Figure 1.10: Comparison of cell viability between two Gram-negative bacteria: *P. aeruginosa* and *E. coli* in 24 h biofilm.

The effect of B-G activity towards eukaryotic cells was also examined using NIH3T3 mouse fibroblast cells. These mammalian cells are approximately 20 µm and are way larger than bacterial cells (1-2 µm). Under SEM, no mechanical damage of these cells was observed (Fig. 1.11). In the literature, it was mentioned that sodium pentaborate pentahydrate, which is a source of boron, when combined with graphene oxide (GO), enhances adherence and proliferation of mammalian cells [26]. On the other hand, substrates with wrinkles and ripples enhance cell proliferation and viability [27]. Inspite of our B-G membranes having a lot of ripples and wrinkles, which is supposedly for interaction, enhanced proliferation was not observed. It has to be noted that though boron can enhance the proliferation of mammalian cells, the structural morphology, function and properties of mouse fibroblast cells used in this experiment and mesenchymal stem cells used in above mentioned literature study are quite different. The negative control (bacterial cells on glass coverslip) showed that incubation conditions did not cause morphological damages.

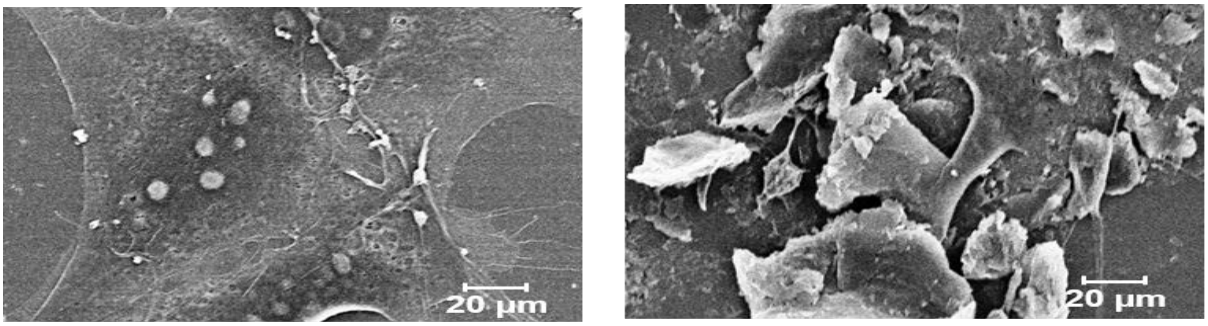

Figure 1.11: SEM images of NIH3T3 mouse fibroblasts on control (left) and boron doped graphene membrane (right).

1.3.3. Boron doped graphene on different substrates

Some studies suggest that the antibacterial activity of graphene-based nanostructures depend on the type of the substrate graphene is present on i.e. conductor, semi-conductor or insulator. It was reported that the antimicrobial activity of CVD-graphene is dependent on the substrate conductivity where maximum effect was observed with conducting substrates followed by semi-conductors and negligible effect with insulators [28]. In our experiments, a similar approach was tried with B-G membranes prepared on gold, silicon dioxide and silicon substrates with both Gram-positive *S. epidermidis* and Gram-negative *P. aeruginosa.* SEM image analysis of *S. epidermidis* and *P. aeruginosa* 24 h biofilm showed that there is no evidence of significant membrane damage on these substrates (Fig. 1.12).

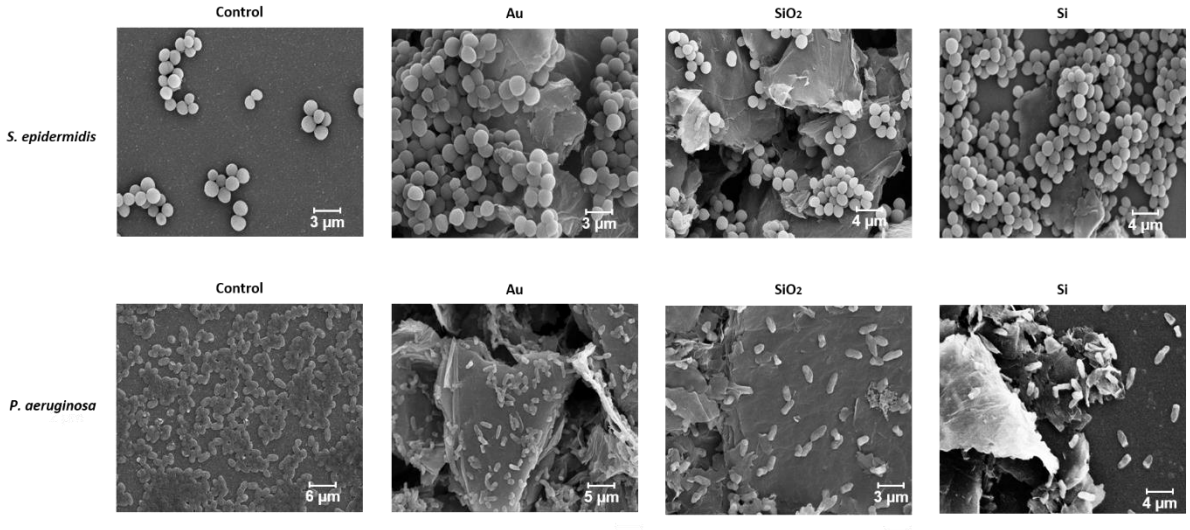

Figure 1.12: SEM images of Gram-positive *S. epidermidis* and Gram-negative *P. aeruginosa* on control and boron doped graphene membranes on Au, SiO_2 and Si.

1.4. Conclusion

Both Gram-positive and Gram-negative bacteria showed no evident membrane damage and cell death on B-G. Also, B-G on different substrates did not show any different antibacterial activity. This indicates that the surface of B-G cannot significantly destroy microbes. On the other side B-G enhanced secretion of exotoxin A (tox A) of *P. aeruginosa*. Tox A has potential use in cancer and hepatitis B treatment.

2. Antibacterial activity of other 2D materials

2.1. Introduction

Since the discovery of graphene and exploring its unique properties, 2D materials such as chalcogenides, transition metal oxides have gained tremendous research interest [29]. A single layer of transition metal dichalcogenides (TMDs) consist of two planes of hexagonal arranged chalcogen atoms (X) linked to hexagonal plane of metal atom (M), with stoichiometry MX_2. The atoms are held together by weak Van der Waals forces. Depending on the combination of chalcogen and metal atoms, various types of TMDs can occur. WS_2 and MoS_2 are prototypical TMDs. Due to their semiconducting properties and tunable gap, WS_2 and MoS_2 have been identified as graphene analogue materials [30]. They are promising materials with a wide range of potential applications including energy generation, catalysts, sensing and biomedicine. MoS_2 sheets can be used in biomedical applications for detection of DNA molecules [31], however, their antibacterial properties are still unexplored.

2.2. Materials and Methods

2.2.1. Materials

MoS_2 and WS_2 in ultrafine powder- and nanoflake solution-forms were obtained from Graphene Supermarket (USA). If not stated differently, all other chemicals used were purchased from VWR BDH Chemicals (UK), EMD Millipore (USA) or Sigma-Aldrich (USA) with the highest purity available.

2.2.2. Preparation of membranes and choosing the right solvent

MoS_2 (Molybdenum disulfide) and WS_2 (Tungsten disulfide) in liquid and powder forms were tested for uniform membrane preparation. As suggested in the literature, acetone, ethanol and isopropyl alcohol (IPA) were used as potential solvents that facilitate uniform distribution of MoS_2- and WS_2-dry powders on glass coverslips [32]. Membranes were first fabricated by using spray drying and spin coating methods only to realize that there was no uniformity in MoS_2- and WS_2 dispersion. By using drop casting method, MoS_2 and WS_2 membranes were successfully fabricated on glass coverslips. Dispersed solutions of MoS_2 and WS_2 flakes in

different concentrations (1, 2 and 4 mg/ml) were sonicated for 30 min prior to drop casting, glass coverslips were cleaned with acetone and ethanol (70%). Few drops of MoS_2 and WS_2 were casted on separate glass slides and left overnight for drying, followed by heat treatment (180°C, 2 h). MoS_2 and WS_2 in liquid form was casted as single and double layer. After optical and SEM characterization of the fabricated membranes, it was realized that the samples with MoS_2 and WS_2 dispersed in IPA provided the most uniform membranes, which were used for further experiments. The antibacterial testing on these membranes was performed in the same way as for B-G membranes (see page 13, 14). Used solvents for MoS_2 and WS_2 membranes and their parameters are summarized in Table 2.1.

Table 2.1: Solvents used for membrane formation with MoS_2 (Molybdenum disulfide) and WS_2 (Tungsten disulfide). ☑ - successful, ☒ - non-successful.

Material	**Solvent**	**Membrane uniformity**	**Membrane conductivity**	**Biofilm stability**
WS_2, MoS_2 (dry powder)	Ethanol	☒	☒	☒
	Acetone	☑	☑	☒
	IPA	☑	☑	☑

2.3. Results and Discussion

The antibacterial activities of graphene analogue MoS_2 and WS_2 were tested. Some studies claim that graphene oxide-MoS_2 nanosheets show antibacterial effect towards Gram-negative bacteria like *E. coli*, due to induction of oxidative stress [33]. However, membranes prepared from both 2D materials did not have any antibacterial effect towards Gram-positive as well as Gram-negative bacteria. Under SEM evaluation no morphological changes were observed (Fig. 2.1, 2.2). Moreover, surfaces with MoS_2 had no observable effect on *P. aeruginosa* viability (Fig. 2.3).

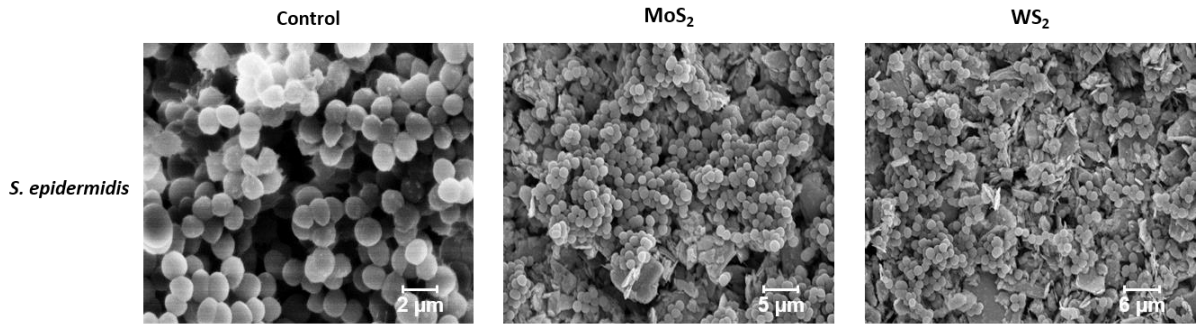

Figure 2.1: SEM images of Gram-positive *S. epidermidis* on control and MoS_2, WS_2 membranes.

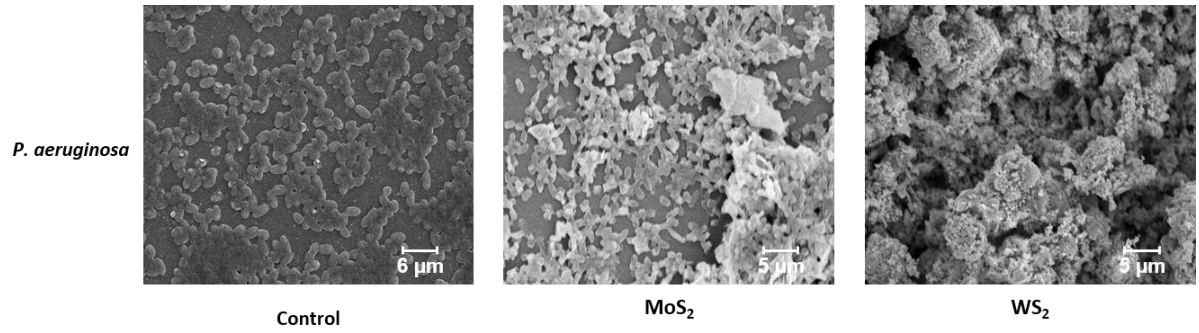

Figure 2.2: SEM images of Gram-negative *P. aeruginosa* on control and MoS_2, WS_2 membranes.

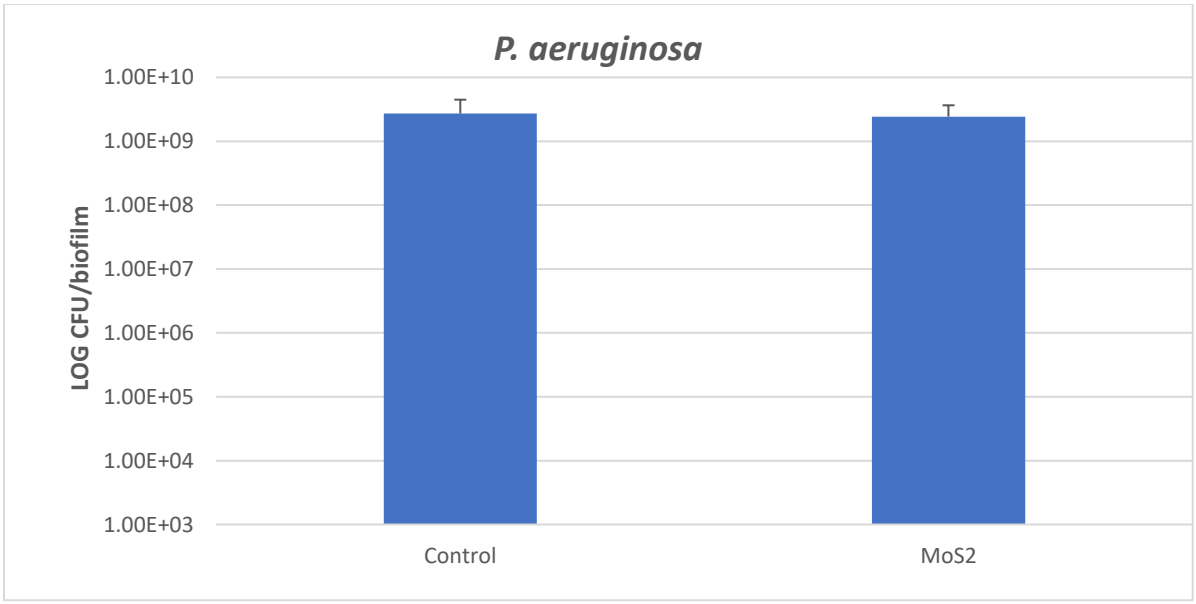

Figure 2.3: The viable *P. aeruginosa* cells in 24 h biofilm on MoS_2 membrane compared to control sample (glass coverslip).

3. Enhanced secretion of Exotoxin A by *P. aeruginosa* on boron doped graphene membranes

3.1. Materials and methods

3.1.1. RNA isolation

P. aeruginosa 24 h biofilm cells grown on coverslips and held in 12-well plates, were submerged by 1 ml of RNA Later solution and kept in the refrigerator. To further process the samples, RNA Later solution was diluted 1:1 with RNAse-free water and centrifuged (23,000 g, 10 min, 4°C) to pellet the bacteria. The pellets were then kept in dry ice until ready for extraction, according to the RNAsnap method for Gram-negative bacteria [34]. Briefly, the pellets were vortex-re-suspended in 100 µl of RNA extraction solution with 18 mM EDTA, 0.025% SDS, 1% 2-mercaptoethanol and 95% RNA-grade formamide. Bacteria were then lysed by incubation in a thermoblock (95°C, 7 min). After centrifugation (16,000 g, room temperature), the RNA-containing supernatant was transferred to a fresh tube, without disturbing the clear gelatinous pellet containing protein, cell debris and DNA, and finally stored at -80°C.

3.1.2. Reverse transcription and semi-quantitative Real Time Polymerase Chain Reaction (RT-PCR)

The amount of total RNA was determined by measuring A_{260} with a Nanodrop 1000 (Thermo Scientific, USA), using the RNA extraction solution as a blank. Due to the chemical composition of the RNAsnap supernatant, a standard sodium acetate/ethanol precipitation step was required, before reverse transcription can occur. Equal amounts of total RNA from each sample were then reverse transcribed into cDNA at once, using a High-Capacity cDNA Reverse Transcription Kit (Thermo Scientific, USA), random hexamers and according to the manufacturer's protocol. A semi-quantitative RT-PCRs [35] with 25/30/35 amplification cycles were performed to assess the relative expression rate of tox A and 16S rRNA, the latter for normalization purposes. A Phusion™ Hot Start II High-Fidelity DNA polymerase kit (Thermo Scientific, USA) was used, following the provided protocol. Primers used were as follows: 16SrRNA-Fwd: 5'-CAAAACTACTGAGCTAGAGTACG-3', 16SrRNA-Rev: 5'-

TAAGATCTCAAGGATCCCAACGGCT-3', ToxA-Fwd: 5'-ATGGTGTAGATCGGCGACAT-3', ToxA-Rev: 5'-AAGCCTTCGACCTCTGGAAC-3'.

3.2. Results and discussion

P. aeruginosa, which was tested for the antibacterial activity of B-G, resulted in an interesting observation where inspite of not being antibacterial, B-G was found to enhance EPS secretion (Fig. 3.1). The samples were successfully tested in enrichment of tox A. cDNA of all the *P. aeruginosa* samples (4-, 8- and 24 h biofilm) was equaly loaded after reverse transcription using 16S rRNA gene (Fig 3.2). From densitometric analysis of the semi-quantitative RT-PCR a 2.6-fold increase in the levels of tox A expression compared to control (uncoated coverslips) was observed (Fig. 3.3). Figure 3.3 shows a no-template control (NTC, the same RNA without reverse transcription) and two technical replicates for each of the glass only and B-G coated coverslips.

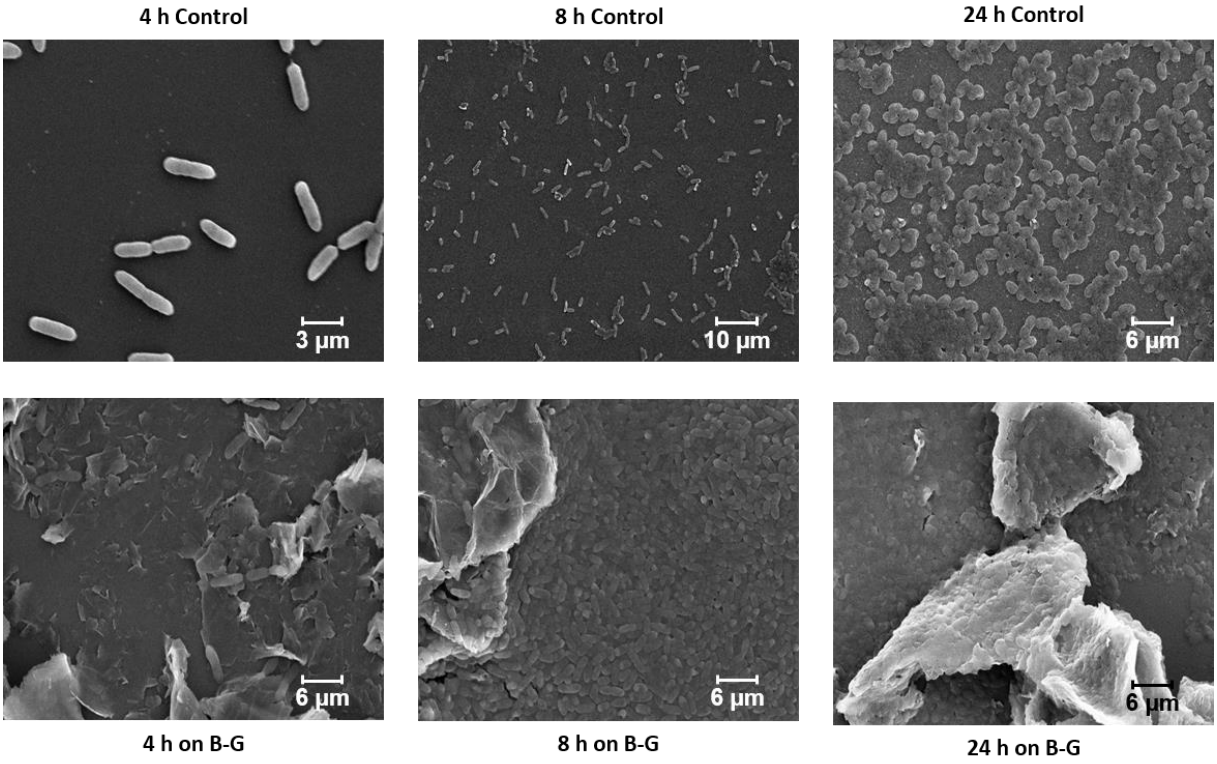

Figure 3.1: SEM images of *P. aeruginosa* 4, 8 and 24 h biofilm on control and boron doped graphene membranes.

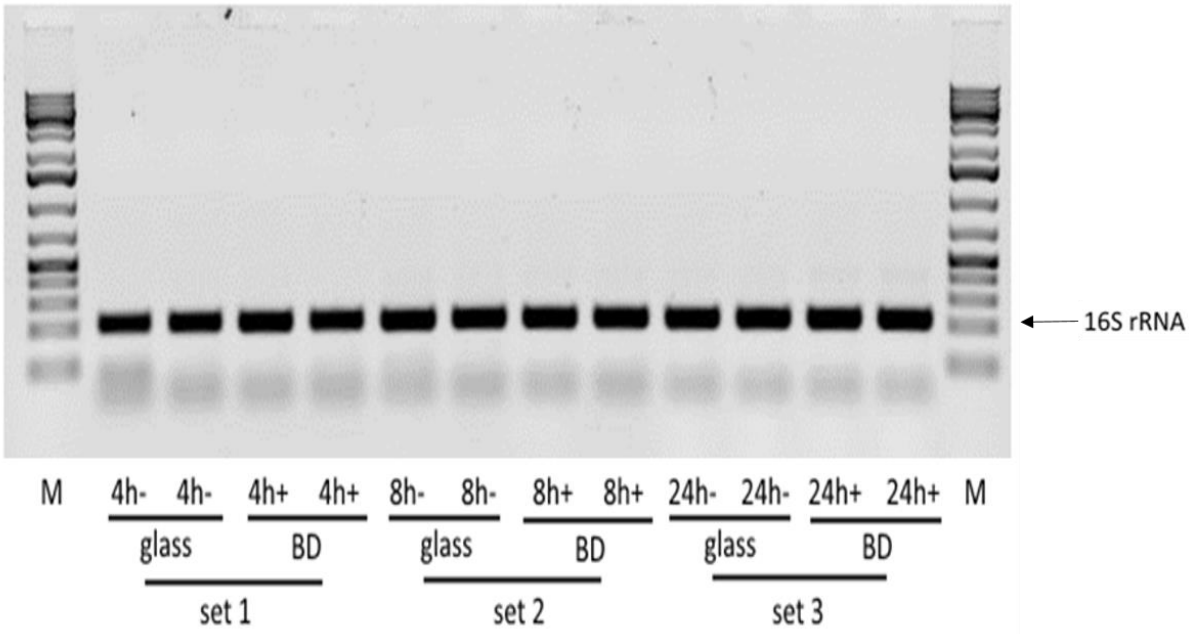

Figure 3.2*:* RT-PCR with identical settings on 16S rRNA cDNA, as an internal normalization reference. Marker: GeneRuler 1 kb Plus DNA Ladder 75-20000 bp (Thermo Scientific, USA)-

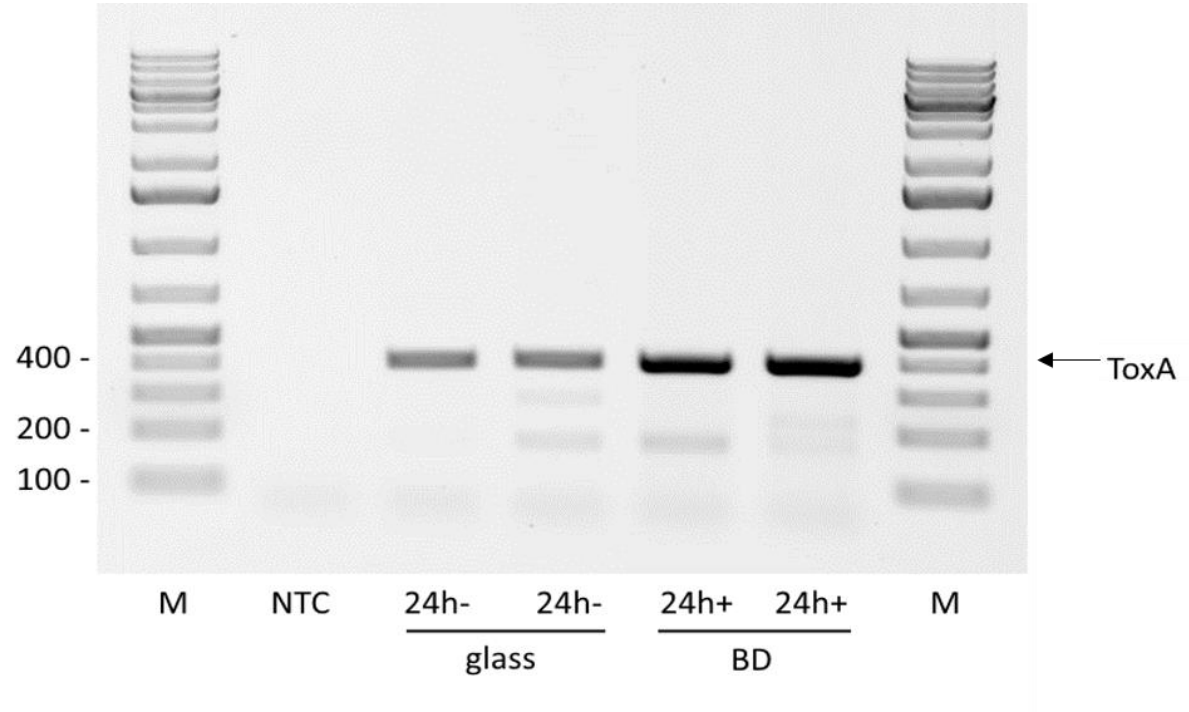

Figure 3.3*:* Semi-quantitative RT-PCR and normalization of data: RT-PCR after 30 cycles, showing the 2.6-fold overexpression of Tox A, after 24 h of growth, in presence of boron doped graphene. Marker: GeneRuler 1 kb Plus DNA Ladder 75-20000 bp (Thermo Scientific, USA).

4. Antibacterial activity of plant and bacteria derived nanoparticles

4.1. Introduction

Metal nanoparticles have attracted interest of scientists, since implementation of nanotechnology allows the synthesis of particles in nanometers [36]. Due to their high surface area to volume ratio and unique physicochemical and biological properties, the use of NPS in electrical, chemical or biological field has attracted global attention. Silver ions show high toxicity against microorganisms. There are several chemical and physical methods for the production of nanoparticles. These existing methods are usually expensive, labor extensive and potentially hazardous to the surrounding environment as well as living organisms. Hence, researchers are using alternative ways to produce metallic nanoparticles which are easy, cheap and non hazardous. In this study silver and gold nanoparticles were produced by using plant extracts and bacteria which have the ability to reduce silver and gold salt to respective nanoparticles. Silver has been used in medical field for treatment of wounds, burns and bacterial infections [37, 38]. Silver in nanoparticle shows enhanced antibacterial activity. The antibacterial efficacy of gold nanoparticles (CS-Au-NPs) and silver nanoparticles (CS-Ag-NPS) by *Cannabis sativa* (*C. sativa*) (Hemp) was evaluated by determining minimum growth inhibitory concentration (MIC) and minimum bactericidal concentration (MBC) against Gram-positive and Gram-negative bacteria.

4.2. Materials and Methods

4.2.1. Synthesis of nanoparticles

Eco-friendly synthesis of nanoparticles has been gaining a lot of importance due to its environment friendly approach. In this study, silver and gold nanoparticles were produced by *C. sativa* which have the ability to reduce silver and gold salts to respective nanoparticles. The antibacterial activity was evaluated by determining the MIC and MBC towards the following bacterial strains: *Pseudomonas aeruginosa* PA01, *E. coli* (UTI89) and *S. epidermidis* (ATCC 35984). All strains are classified to risk group 2 in biosafety guidelines. Moreover, the

antibacterial activity was confirmed by colony forming units counting (CFUs), scanning electron microscopy (SEM) and live /dead staining.

4.2.2. Determination of Minimum Inhibitory Concentration (MIC) and Minimum Bactericidal Concentration (MBC)

MIC is the lowest concertation of material that inhibits visible growth of bacteria after overnight incubation. Experiments were performed in 96-well plates. NPs were suspended in dH_20 (1 mg/ml) and sonicated for 15 min prior to use, followed by serial dilution in LB broth media (total volume 180 µl) ranging from 6.25 µg/ml to 50 µg/ml. Bacterial culture in a logarithmic phase (20 µl) was added to serial dilutions of NPs. The 96-well plates were incubated with shaking (170 rpm, 37°C) on IKA KS 4000i Control Shaking Incubator (IKA-Werke GmbH & Co. KG, Staufen, Germany) overnight. MIC was determined when no turbidity in the wells was observed. After the MIC determination of NPs, the aliquots of cultures where no growth was observed, were plated on LB-agar and incubated at 37°C for 24 h. MBC is defined as the lowest concentration of material required to kill bacterial population

4.2.3. Colony Forming Units (CFUs)

Biofilms were grown for 24 h without any disturbance (See 1.2.6.). After the 24 h old culture medium was replaced with different concentration of AgNP containing fresh medium and incubated for another 24 h. After 24 h of nanoparticle treatment, biofilms were homogenized by sonication and plated on agar plates for CFU counting.

4.2.4. Live Dead Staining

The toxicity of CS-Ag-NPs to the surfaces for *P. aeruginosa* and *E. coli* cells was tested by staining the cells (24 h biofilm) with a membrane integrity evaluation kit (ReadyProbes® Cell Viability Imaging Kit Blue/Red, Thermo Scientific, USA). Its active dyes show different specificities within viable and damaged cells, with NucBlue® Live reagent staining the nuclei of all the cells, while propidium iodide stains only the nuclei of cells with compromised membrane integrity. After treating the biofilm with different concentration of AgNPs, as described above, bacterial cells were stained according to the kit manufacturer's instructions and fixed with freshly made 4% paraformaldehyde in DPBS for 10 min at room temperature.

The samples were then rinsed in distilled water and mounted with a droplet of ProLong® Diamond Antifade Mountant medium (Thermo Scientific, USA) against a glass coverslip and the back of the coverslip attached, with a small amount of superglue, to a glass slide for imaging. Imaging was performed with a confocal laser scanning microscope (LSM 700 NLO, Carl Zeiss, Germany). For all samples three biological replicates were analyzed, with five images analyzed per replicate. Representative images are shown.

4.2.5. Scanning Electron Microscopy (SEM)

Biofilms were grown for 24 h without any disturbance. After the 24 h old culture medium was replaced with different concentration of AgNP containing fresh medium and incubated for another 24 h. After 24 h of nanoparticle treatment biofilms, were fixed with gluteraldehyde, dehydrated with graded ethanol and imaging was performed by using SEM after gold coating (see 1.2.10.).

4.3. Results and discussion

The determined MIC and MBC values of NPs against 3 different bacterial strains are shown in Table 4.1. S*. epidermidis* showed resistance against CS-Ag-NPs. CS-Ag-NPs showed strong inhibitory as well as bactericidal effect against *P. aeruginosa* and *E. coli.* While *P. aeruginosa* showed MIC value of 6.25 µg/ml*, E. coli* showed the MIC value of 12.5 µg/ml. Obtained MBC value for *E. coli* was 25 µg/ml, while for *P. aeruginosa* 12.5 µg/ml.

Table 4.1: Minimum inhibitory concentration (MIC) and minimum bactericidal concentration (MBC) of CS-Ag-NPs.

Bacteria	**MIC [µg/ml]**	**MBC [µg/ml]**
P. aeruginosa PA01	6.25	12.5
E. coli UT189	12.5	25
S. epidermidis	>50	>50

The MIC and MBC of gold nanoparticles was >50 µg/ml against above mentioned bacteria.

In Figures 4.1 and 4.2 the results from CFUs counting demonstrate loss of cell viability in *P. aeruginosa* and *E. coli* biofilms treated with different concentrations of CS-Ag-NPs.

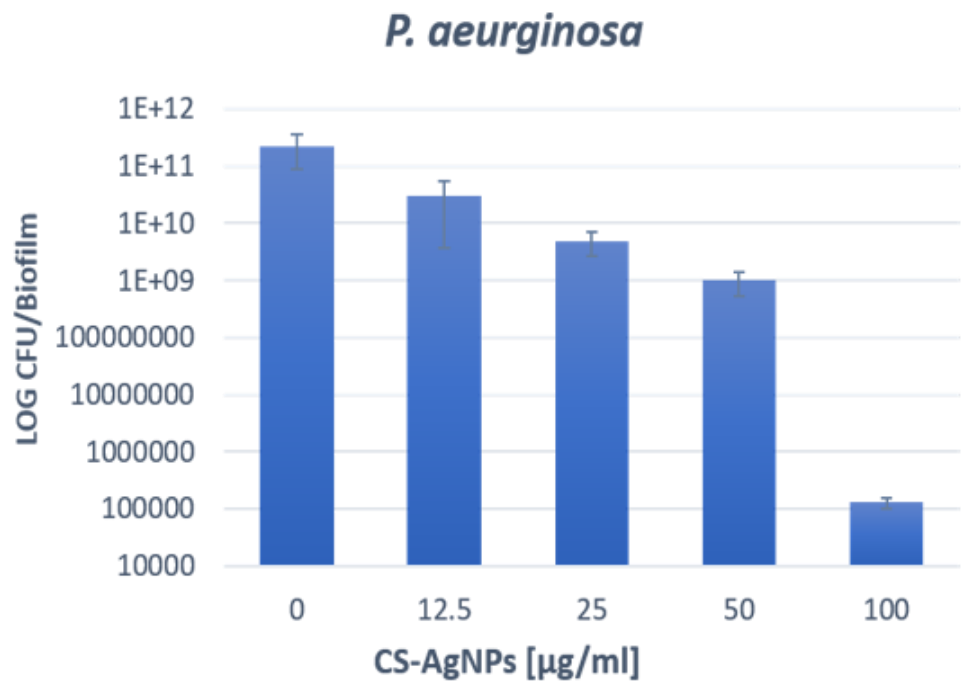

Figure 4.1: The viable *P. aeruginosa* cells in 24 h old biofilm treated with different concentrations of CS-Ag-NPs.

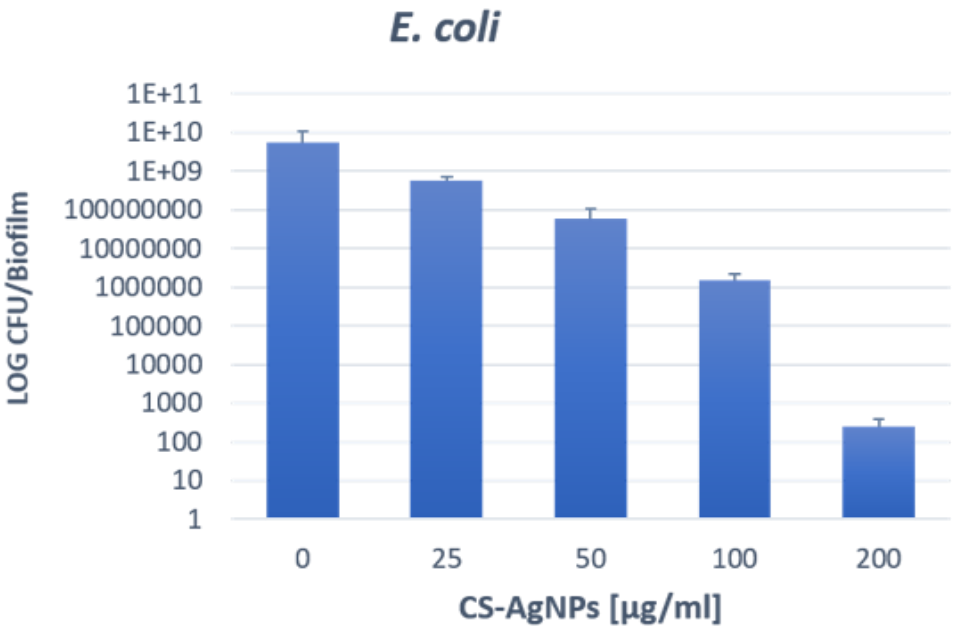

Figure 4.2: The viable *E. coli* cells in 24 h old biofilm treated with different concentrations of CS-Ag-NPs.

In Figures 4.3 and 4.4 the results from fluorescence imaging of bacterial biofilms with live/dead staining showed high bactericidal effect of CS-Ag-NPs against Gram-negative bacteria *P. aeruginosa* and *E. coli*. The number of dead bacterial cells significantly increased in biofilms subjected to CS-Ag-NPs. Higher concentration of CS-Ag-NPs was needed to kill *E. coli* cells compared to *P. aeruginosa*.

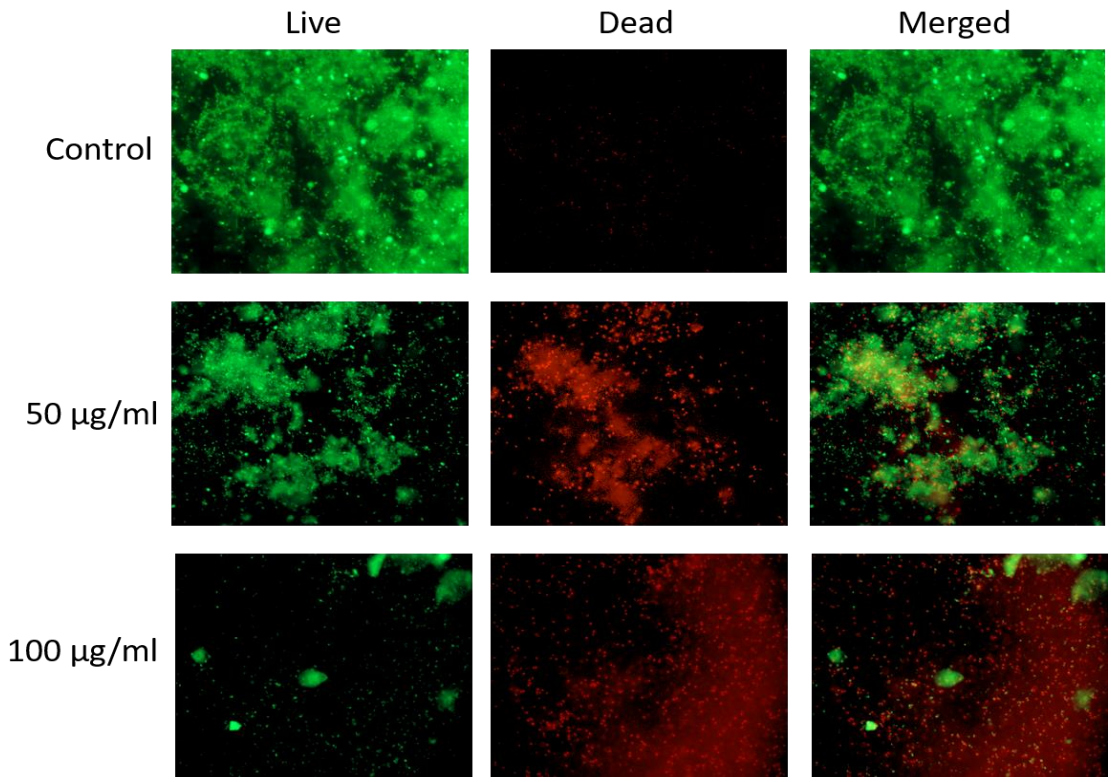

Figure 4.3: Images of live/dead fluorescent staining of *P. aeruginosa* biofilms treated with different concentration of CS-Ag-NPs. The live bacteria are green and the dead bacteria are red.

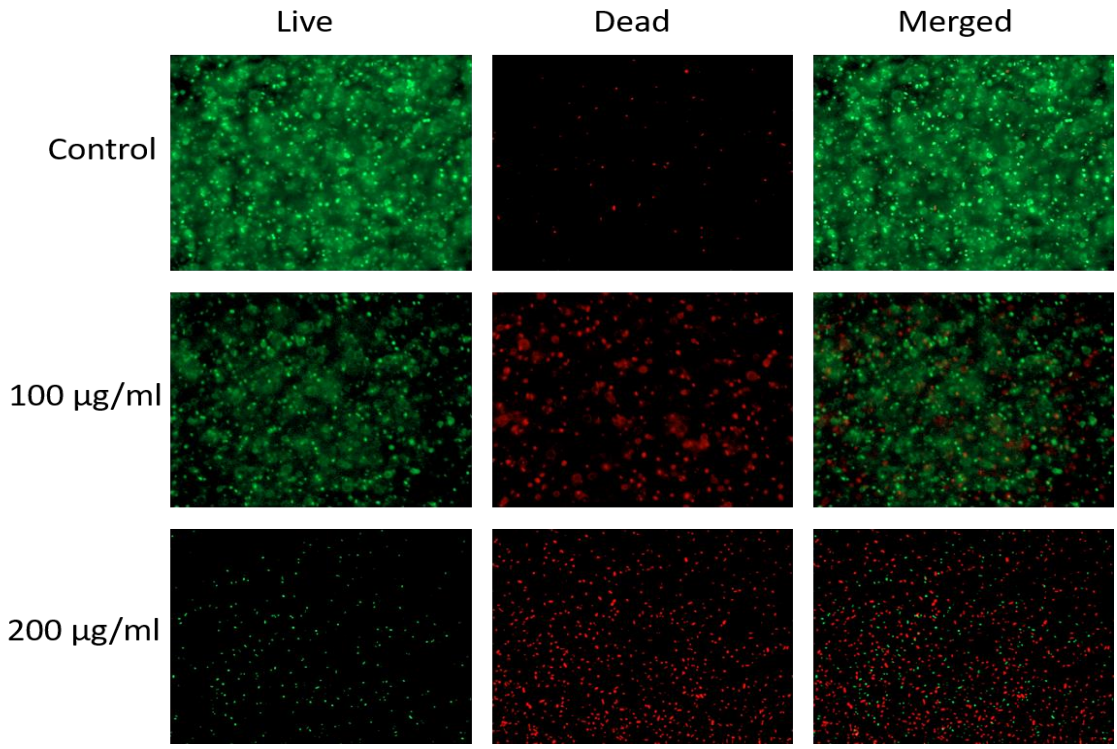

Figure 4.4: Images of live/dead fluorescent staining of *E. coli* biofilms treated with different concentration of CS-Ag-NPs. The live bacteria are green and the dead bacteria are red.

From the SEM images shown in Figures 4.5 and 4.6, clear morphological changes in bacterial shape can be seen, if they have been subjected to CS-Ag-NPs.

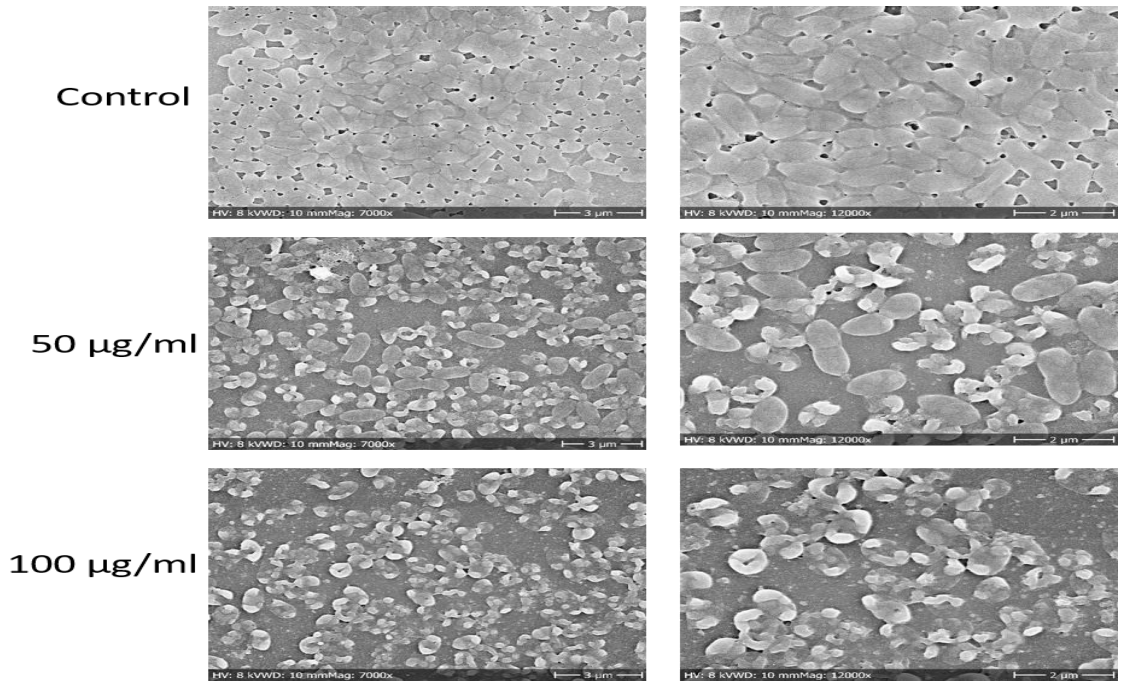

Figure 4.5: SEM images of *P. aeruginosa* 24 h biofilm subjected to different concentrations of CS-Ag-NPs.

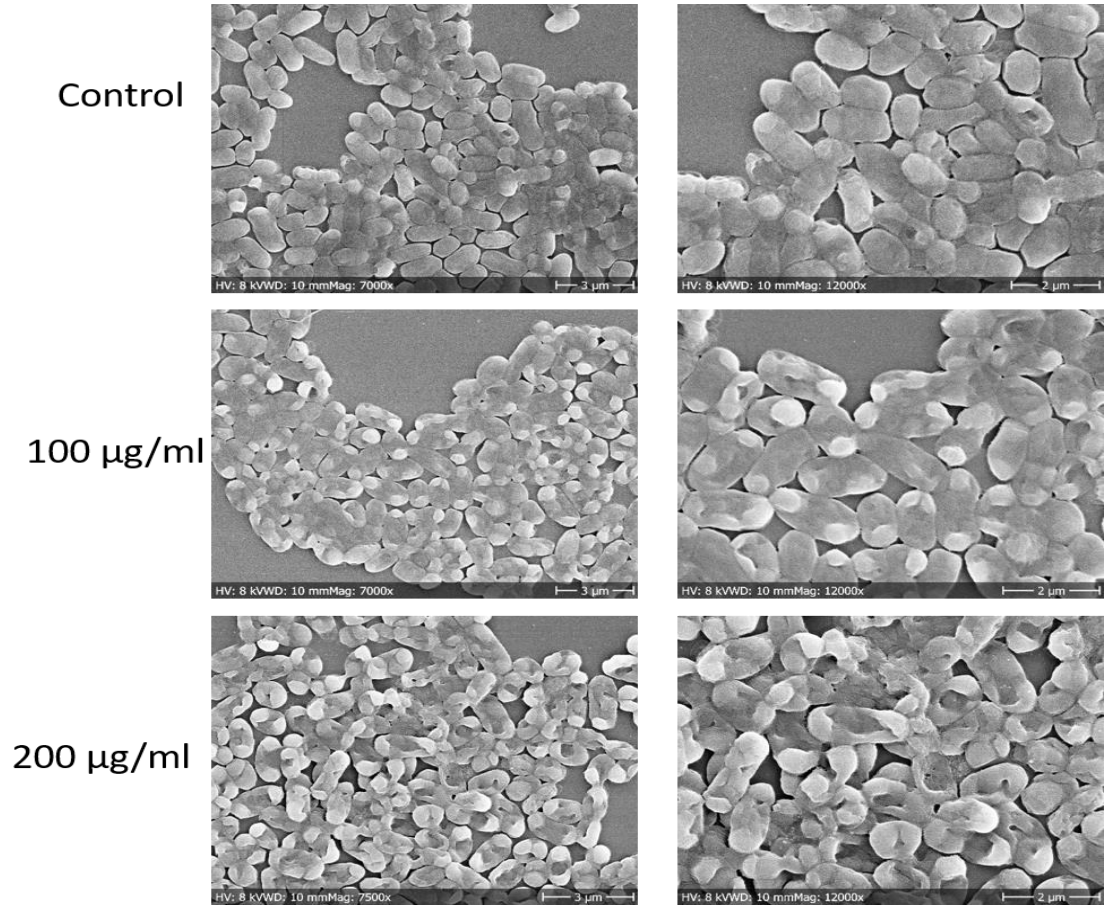

Figure 4.6: SEM images of *E. coli 24* h biofilm subjected to different concentrations of CS-Ag-NPs.

4.4. Conclusion

For the 3 strains, all experiments were independently performed 2 times and similar results were obtained. Evaluation of antibacterial effect of nanoparticles was done according to standard protocol. Silver nanoparticles from *Cannabis sativa* showed toxicity against tested Gram-negative bacteria. There was an increased antibacterial activity with increasing nanoparticle concentrations. Gold nanoparticles from *C. sativa* did not show neither bacteriostatic nor bactericidal activity. Further experiments are needed to confirm how these nanoparticles are killing the bacterial cells.

5. Bacterial biofilm sensor

5.1. Introduction

The project was primarily based on detecting bacterial biofilm on implants and other medical devices. The devices were fabricated by standard photolithography and etching techniques after CVD monolayer graphene transfer. Lab view was used for coding. A user-friendly interface was used to connect the chip with a holder for electrical measurements.

The chips were placed in bacterial solution and real-time data was collected by applying voltage and current through the chip. Gram-positive bacteria *S. epidermidis* was used for testing. The resistance values at the starting point and after different time periods were compared and analyzed graphically. Typically, it took 4 h for a bacterial biofilm to start to grow in detectable quantities. As the biofilm grows thicker the resistance also increases. In this way, we work with different bacterial solutions, time frames, and current to sense the biofilm formation using graphene based sensor. Figure 1. shows the setup of the customized holder and the fabricated chip.

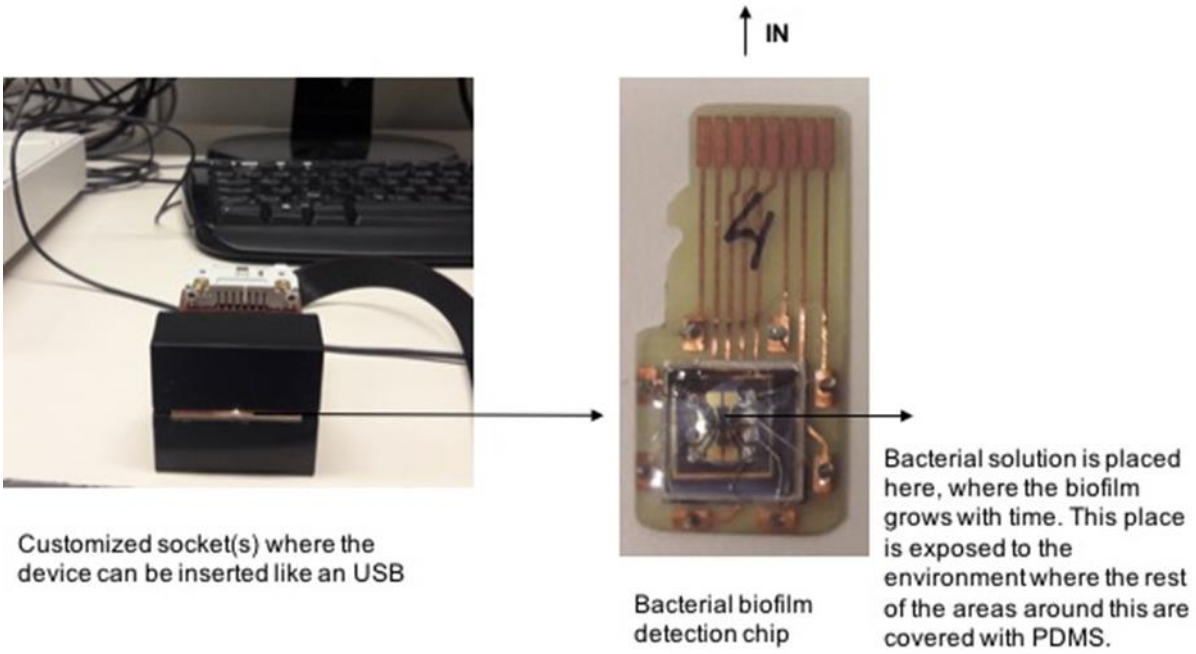

Figure 5.1: Setup of the customized holder (left) and the fabricated chip (right). USB – Universal Serial Bus. PDMS – Polydimethylsiloxane.

5.2. Materials and Methods

After the fabrication and testing of the device, firstly the chip was placed in the holder and calibrated using standard dH_2O. Further, as a control, the chip was dipped into the control medium (without bacteria) and run for 6 h. Real-time data was acquired using lab view interface. In the next step, bacterial suspension with the medium was run for another 6 h and the data was collected.

5.3. Results and discussion

A graph is plotted against time and resistance (Fig. 5.2.) where the difference between the two graphs can be clearly observed (one with only medium and the second with medium + bacteria). We got different patterns when chip was placed in only medium compared to medium with *S. epidermidis*. In control sample there is no change in resistance with time. As the bacterial biofilm starts growing with time, the resistance of the chip increases.
Further experimental studies are needed in order to study change in resistance with biofilm growth, where it might correlate to different bacterial strains.

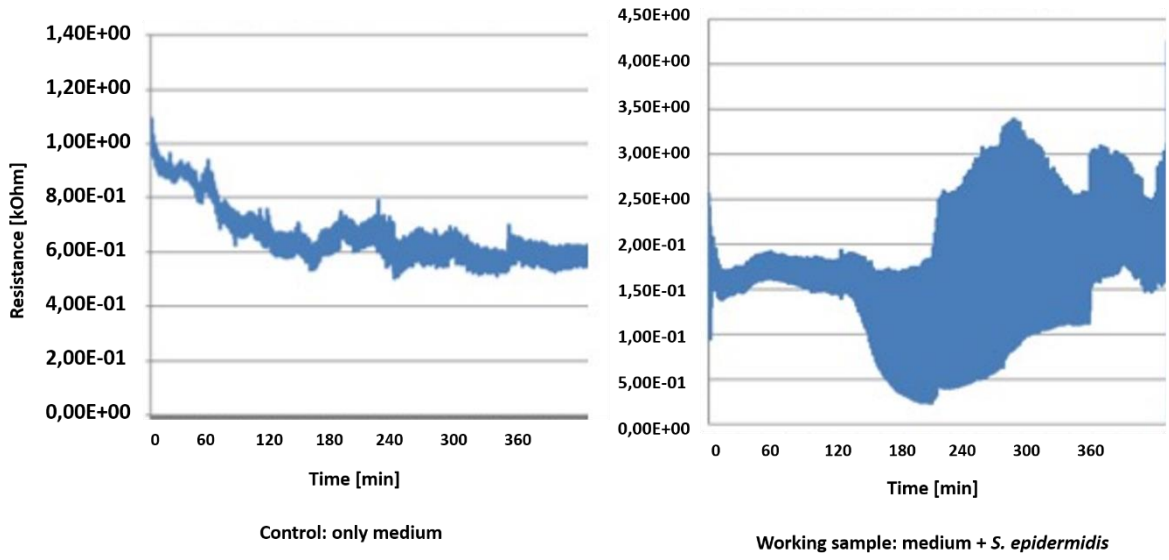

Figure 5.2: Graphs showing the difference in resistance values between the control and the working sample.

6. Literature

1. Neto, A. C., Guinea, F., Peres, N. M., Novoselov, K. S., & Geim, A. K. (2009). The electronic properties of graphene. *Reviews of modern physics*, *81*(1), 109.
2. Geim, A. K., & Novoselov, K. S. (2007). The rise of graphene. *Nature materials*, *6*(3), 183-191.
3. Liu, J., Cui, L., & Losic, D. (2013). Graphene and graphene oxide as new nanocarriers for drug delivery applications. *Acta biomaterialia*, *9*(12), 9243-9257.
4. Mao, H. Y., Laurent, S., Chen, W., Akhavan, O., Imani, M., Ashkarran, A. A., & Mahmoudi, M. (2013). Graphene: promises, facts, opportunities, and challenges in nanomedicine. *Chemical reviews*, *113*(5), 3407-3424.
5. Goenka, S., Sant, V., & Sant, S. (2014). Graphene-based nanomaterials for drug delivery and tissue engineering. *Journal of Controlled Release*, *173*, 75-88.
6. Novoselov, K. S., Geim, A. K., Morozov, S. V., Jiang, D., Zhang, Y., Dubonos, S. V., Firsov, A. A. (2004). Electric field effect in atomically thin carbon films. *science*, *306*(5696), 666-669.
7. Chen, X., Zhang, L., & Chen, S. (2015). Large area CVD growth of graphene. *Synthetic Metals*, *210*, 95-108.
8. Zhang, Y. I., Zhang, L., & Zhou, C. (2013). Review of chemical vapor deposition of graphene and related applications. *Accounts of chemical research*, *46*(10), 2329-2339.
9. Chung, C., Kim, Y. K., Shin, D., Ryoo, S. R., Hong, B. H., & Min, D. H. (2013). Biomedical applications of graphene and graphene oxide. *Accounts of chemical research*, *46*(10), 2211-2224.
10. Agnoli, S., & Favaro, M. (2016). Doping graphene with boron: a review of synthesis methods, physicochemical characterization, and emerging applications. *Journal of Materials Chemistry A*, *4*(14), 5002-5025.
11. Thirumal, V., Pandurangan, A., Jayavel, R., & Ilangovan, R. (2016). Synthesis and characterization of boron doped graphene nanosheets for supercapacitor applications. *Synthetic Metals*, *220*, 524-532.
12. Rao, C. N. R., Gopalakrishnan, K., & Govindaraj, A. (2014). Synthesis, properties and applications of graphene doped with boron, nitrogen and other elements. *Nano Today*, *9*(3), 324-343.

13. Bolaños, L., Lukaszewski, K., Bonilla, I., & Blevins, D. (2004). Why boron? *Plant Physiology and Biochemistry*, *42*(11), 907-912.
14. Nielsen, F. H., & Meacham, S. L. (2011). Growing evidence for human health benefits of boron. *Journal of Evidence-Based Complementary & Alternative Medicine*, *16*(3), 169-180.
15. Pizzorno, L. (2015). Nothing boring about boron. *Integrative Medicine: A Clinician's Journal*, *14*(4), 35.
16. Osumi, S., Saito, S., Dou, C., Matsuo, K., Kume, K., Yoshikawa, H., Yamaguchi, S. (2016). Boron-doped nanographene: Lewis acidity, redox properties, and battery electrode performance. *Chemical Science*, *7*(1), 219-227.
17. Nanda, S. S., An, S. S. A., & Yi, D. K. (2015). Oxidative stress and antibacterial properties of a graphene oxide-cystamine nanohybrid. *International journal of nanomedicine*, *10*, 549.
18. Rojas-Andrade, M. D., Chata, G., Rouholiman, D., Liu, J., Saltikov, C., & Chen, S. (2017). Antibacterial mechanisms of graphene-based composite nanomaterials. *Nanoscale*, *9*(3), 994-1006.
19. Applerot, G., Lellouche, J., Lipovsky, A., Nitzan, Y., Lubart, R., Gedanken, A., & Banin, E. (2012). Understanding the antibacterial mechanism of CuO nanoparticles: revealing the route of induced oxidative stress. *Small*, *8*(21), 3326-3337.
20. Li, J., Wang, G., Zhu, H., Zhang, M., Zheng, X., Di, Z., Wang, X. (2014). Antibacterial activity of large-area monolayer graphene film manipulated by charge transfer. *Scientific reports*, *4*.
21. Akhavan, O., Ghaderi, E., & Esfandiar, A. (2011). Wrapping bacteria by graphene nanosheets for isolation from environment, reactivation by sonication, and inactivation by near-infrared irradiation. *The Journal of Physical Chemistry B*, *115*(19), 6279-6288.
22. Donlan, R. M., & Costerton, J. W. (2002). Biofilms: survival mechanisms of clinically relevant microorganisms. *Clinical microbiology reviews*, *15*(2), 167-193.
23. Stewart, P. S., & Costerton, J. W. (2001). Antibiotic resistance of bacteria in biofilms. *The lancet*, *358*(9276), 135-138.

24. Tennyson, W. D., Tian, M., Papandrew, A. B., Rouleau, C. M., Puretzky, A. A., Sneed, B. T., & Geohegan, D. B. (2017). Bottom up synthesis of boron-doped graphene for stable intermediate temperature fuel cell electrodes. *Carbon*, *123*, 605-615.
25. Hafkemeyer, P., Brinkmann, U., Brinkmann, E., Pastan, I., Blum, H. E., & Baumert, T. F. (2008). Pseudomonas exotoxin antisense RNA selectively kills hepatitis B virus infected cells. *World Journal of Gastroenterology: WJG*, *14*(18), 2810.
26. Taşlı, P. N., Doğan, A., Demirci, S., & Şahin, F. (2016). Myogenic and neurogenic differentiation of human tooth germ stem cells (hTGSCs) are regulated by pluronic block copolymers. *Cytotechnology*, *68*(2), 319-329.
27. Dulgar-Tulloch, A. J., Bizios, R., & Siegel, R. W. (2009). Human mesenchymal stem cell adhesion and proliferation in response to ceramic chemistry and nanoscale topography. *Journal of biomedical materials research Part A*, *90*(2), 586-594.
28. Li, J., Wang, G., Zhu, H., Zhang, M., Zheng, X., Di, Z., Wang, X. (2014). Antibacterial activity of large-area monolayer graphene film manipulated by charge transfer. *Scientific reports*, *4*.
29. Radisavljevic, B., Radenovic, A., Brivio, J., Giacometti, I. V., & Kis, A. (2011). Single-layer MoS2 transistors. *Nature nanotechnology*, *6*(3), 147-150.
30. Xu, M., Liang, T., Shi, M., & Chen, H. (2013). Graphene-like two-dimensional materials. *Chemical reviews*, *113*(5), 3766-3798.
31. Zhu, C., Zeng, Z., Li, H., Li, F., Fan, C., & Zhang, H. (2013). Single-layer MoS2-based nanoprobes for homogeneous detection of biomolecules. *Journal of the American Chemical Society*, *135*(16), 5998-6001.
32. Chua, X. J., & Pumera, M. (2017). The effect of varying solvents for MoS 2 treatment on its catalytic efficiencies for HER and ORR. *Physical Chemistry Chemical Physics*, *19*(9), 6610-6619.
33. Kim, T. I., Kwon, B., Yoon, J., Park, I. J., Bang, G. S., Park, Y., & Choi, S. Y. (2017). Antibacterial Activities of Graphene Oxide–Molybdenum Disulfide Nanocomposite Films. *ACS Applied Materials & Interfaces*, *9*(9), 7908-7917.
34. Stead, M. B., Agrawal, A., Bowden, K. E., Nasir, R., Mohanty, B. K., Meagher, R. B., & Kushner, S. R. (2012). RNA snap™: a rapid, quantitative and inexpensive, method for isolating total RNA from bacteria. *Nucleic acids research*, *40*(20), e156-e156.

35. Marone, M., Mozzetti, S., De Ritis, D., Pierelli, L., & Scambia, G. (2001). Semiquantitative RT-PCR analysis to assess the expression levels of multiple transcripts from the same sample. *Biological procedures online*, *3*(1), 19-25.
36. Singh, P., Kim, Y. J., Wang, C., Mathiyalagan, R., & Yang, D. C. (2016). The development of a green approach for the biosynthesis of silver and gold nanoparticles by using Panax ginseng root extract, and their biological applications. *Artificial cells, nanomedicine, and biotechnology*, *44*(4), 1150-1157.
37. Rai, M., Yadav, A., & Gade, A. (2009). Silver nanoparticles as a new generation of antimicrobials. *Biotechnology advances*, *27*(1), 76-83.
38. Dar, M. A., Ingle, A., & Rai, M. (2013). Enhanced antimicrobial activity of silver nanoparticles synthesized by Cryphonectria sp. evaluated singly and in combination with antibiotics. *Nanomedicine: Nanotechnology, Biology and Medicine*, *9*(1), 105-110.
39. Chua, X. J., & Pumera, M. (2017). The effect of varying solvents for MoS 2 treatment on its catalytic efficiencies for HER and ORR. *Physical Chemistry Chemical Physics*, *19*(9), 6610-6619.